

Velocity structure and hypocentral location of earthquakes by simultaneous inversion method: Application to the area of Kalabagh, Pakistan

M. Qaisar¹, M.B. Shahid², Tariq Mahmood², Karam Khan² and Suhail Ahmad²

¹Center for Earthquake Studies, NCP Quaid-i-Azam University Campus, Islamabad

²Micro Seismic Studies Programme, Islamabad

Abstract

A layered P-wave velocity model in the crust and just below the Moho is estimated for the Kalabagh area. The arrival-time data of p-waves from local earthquakes that occurred within the Kalabagh seismic network operated from March 1981 to September 1990 are used for inversion. A damped least-squares method is applied in the inversion process for determining the hypocenter and velocity parameters simultaneously. The estimated P-wave velocities are 5.33 ± 0.04 and 5.56 ± 0.05 km/s in the upper crust (above a depth of 11km), 6.27 ± 0.03 and 6.57 ± 0.08 km/s in the intermediate crust (from 11 to 25 km of depth) and 6.94 ± 0.09 km/s in the lower crust i.e. up to the Moho discontinuity which is, in this case, at 35.5 km depth. The velocity just below the Moho is found to be 8.00 ± 0.09 km/s. The 90% of relocated events show an epicentral accuracy of the order of 2km or better. Most of the relocated events are found at a depth range of 5 to 20 km, indicating that the active zone lies in this depth range.

Keywords: Simultaneous inversion; Velocity structure; Local earthquake data; Hypocentral location; Kalabagh area.

1. Introduction

The study area encompasses the Potwar region including Salt Range, Surghar Range, and Mianwali depression basin (Fig. 1) that lies south of the Himalayan thrust belt and is one of the advanced parts of the Indian plate (Wadia, 1976). In order to study the seismicity of this area, a seismic network was installed in 1981 around the Kalabagh town. Since then about 700 events have been recorded by this network through September 1990. For further seismic studies of the region, it is important to know the seismic velocity structure beneath the area as accurately as possible as no studies were conducted in the past for the determination of seismic velocity structure beneath the study area. This can be achieved by inverting the first arrival times of micro-earthquakes recorded by the local seismic network with the available inversion methods (Crosson 1976a, 1976b; Aki and Lee, 1976; Pavlis and Booker, 1980; Spencer and Gubbins 1980; Mao, 1989). For detailed review of the different methodologies on inversion of seismic data see Thurber and Aki (1987).

Mao (1989) has used similar techniques as Pavlis and Booker (1980) and Spencer Gubbins (1980) in which hypocenter parameters and velocity parameters are decoupled in the inversion procedure. Following this method the hypocenter and velocity model parameters in 1-D are determined simultaneously along with model parameters perturbation, resolution and covariance for the studied region. A brief summary of the method is given in the following section.

2. Method of analysis

The arrival times of body waves radiated from seismic sources within the seismic network are the basic input for the analysis. Such data contain information regarding the location of those sources and seismic velocity structure of the subsurface along which the waves traveled. We consider N earthquakes occurring within a network recorded by M seismic stations and the total number of hypocenter parameter to be determined is $4N$. If we assume P unknown velocity model parameters, the total number of parameters to be determined in the simultaneous inversion problem are $4N+P$. In an ensemble of

arrival time observations, the arrival time for the i th event at the j th station is,

$$T_{ij} = T_{ij}(X_{1i}, X_{2i}, X_{3i}, X_{4i}, U_1, U_2, \dots, U_p)^T \quad (1)$$

$i = 1, 2, \dots, N$
and $j = 1, 2, \dots, M$

where X_{1i}, \dots are the hypocenter parameters and U_1, \dots are the aggregate of possible parameters describing the velocity model. The station parameters are implicitly involved as independent variables and are indexed by j . Hence quasi-linear equations relating small changes in travel time to small changes of the hypocenter and model parameters, by expanding equation (1) in a Taylor's series and discarding all second and higher order terms, are

$$\delta T_{ij} = r_{ij} = \sum_{k=1}^4 \frac{\partial T_{ij}}{\partial X_{ki}} \delta X_{ki} + \sum_{k=1}^p \frac{\partial T_{ij}}{\partial U_k} \delta U_k \quad (2)$$

Where $r_{ij} = T_{ij}^{obs} - T_{ij}^{cal}$, represents the arrival time residuals $\delta X_{ki} = X_{ki} - X_{ki}^0$ and

$\delta U_k = U_k - U_k^0$. The quantities X_{ki}^0 and U_k^0 are points in hypocenters and model space where partial derivatives are evaluated.

For a simultaneous inversion, the linear equations relating the arrival time residuals vector r and the model parameter changes can be written as (Lee and Stewart, 1981),

$$r = B\delta h + A\delta U \quad (3)$$

Where r is a vector of travel time residuals with dimension L ($= M \times N$), δh is a vector of hypocentral parameters adjustment with dimension $4N$ and δU is a vector of slowness parameter adjustments having dimension P and B denote an $L \times 4N$ matrix related to the derivatives of travel times with respect to hypocentral parameters. The matrix A represent an $L \times P$ matrix related to the derivatives of travel times with respect to seismic slowness of the structural model.

$$B = \begin{pmatrix} B_1 & 0 & 0 & 0 & \dots & \dots & 0 \\ 0 & B_2 & 0 & 0 & \dots & \dots & 0 \\ 0 & 0 & B_3 & 0 & \dots & \dots & 0 \\ \vdots & \vdots & \vdots & \vdots & \vdots & \vdots & \vdots \\ 0 & 0 & 0 & 0 & \dots & \dots & B_n \end{pmatrix}$$

$$A = \begin{pmatrix} A_1 \\ A_2 \\ A_3 \\ \vdots \\ A_n \end{pmatrix} \quad (4)$$

Where B_i, A_i ($i = 1, 2, \dots, N$) are $(M \times 4)$ and $(M \times P)$ sub matrices respectively.

To avoid the complications involved in minimizing $\|r - B\delta h + A\delta U\|^2$ and to save computer time and storage, it is possible to decouple mathematically the hypocentral parameters from the velocity parameters in the inversion procedure (Pavlis and Booker, 1980; Spenser and Gubbins, 1980; Mao, 1989). Hence we have from equation (3) as

$$\delta h = B^+(r - A\delta U) \quad (5)$$

$$\delta U = (OA)^+ Or \quad (6)$$

Where the matrix $O = A^T A^T B B^+$ and $(OA)^+$ represent the Moore-Penrose generalized inverse of a matrix (OA) . In Equation (6), the velocity adjustment determination has no direct relation with the hypocenter adjustment but depends only on current model parameters. However, this does not mean that determination of slowness parameters are independent from hypocentral parameters, but only means it is independent from hypocentral adjustment δh . The hypocenter adjustment can be obtained from slowness adjustment δU . According to the singular value decomposition theorem, the generalized inverse of the matrix B can be written as,

In Equation (6), the velocity adjustment determination has no direct relation with the hypocenter adjustment but depends only on current model parameters. However, this does not mean that determination of slowness parameters are independent from hypocentral parameters, but only means it is independent from hypocentral adjustment δh . The hypocenter adjustment can be obtained from slowness adjustment δU . According to the singular value decomposition theorem, the generalized inverse of the matrix B can be written as,

$$B^+ = VS^{-1}U^T \quad (7)$$

Where U and V are orthogonal matrices with order as $L \times L$ and $4N \times 4N$ respectively and S is a $L \times 4N$ diagonal matrix with off-diagonal elements $S_{ij} = 0$ for $i \neq j$. The diagonal elements consist of non negative square roots (S_i , $i = 1, 2, 3, \dots, 4N$) of the Eigen-values of $B^T B$. The matrix S_i^{-1} is equal to $1/S_i$ only if $S_i > 0$ and $S_i^{-1} = 0$ for $S_i = 0$. This means that the generalized inverse exist, even when the matrix is singular.

In practice, the divergence of the linearization-iteration process is often observed due to numerical errors or very small values of S_i . To avoid such ambiguity and to be sure of the convergence of the iteration process, a method called “damped least-squares” was introduced (Levenberg, 1944; Marquardt, 1963). According to damped least squares method, the matrix B^+ is defined as (Aki and Richard, 1980),

$$B^+ = V \{(S^2 + \Theta^2 I)^{-1} S\} U^T \quad (8)$$

where Θ^2 is an adjustable parameter that controls the trade-off between resolution and variance and usually it is much smaller than the largest singular value of S_i . However, it is desirable to choose Θ^2 as small as possible to achieve maximum resolution, but it must be large enough to obtain appropriate stability along with covariance estimates.

In the case of small Eigen values of the matrix OA , the general damped least-squares method can be used. Due to non-linearity of the problem, the coefficient matrices A and B in equation (3) are functions of the model, and the problem must be solved iteratively. The iterative refinements of the

initial estimates are performed using equations (5) and (6) starting with an initial guess of the velocity model and hypocenters. The choice of initial model is important as final solution obtained from the linearized inversion depends crucially on it. The resolution matrices corresponding to the solution vectors (5) and (6) are,

$$R_h = B^+ B \quad (9)$$

$$R_u = (OA)^+ OA, \quad (10)$$

which linearly relate the true solution to the estimated solution. Each component of the model parameter vector is perfectly resolved and gives a unique solution if the resolution matrix is an identity matrix (Wiggins, 1972; Menke, 1984). However, due to uncertainties in our model and data, a unique solution may not be obtained. The following covariance matrices are introduced in the inversion process to check the accuracy of the inversion results,

$$C_h = \sigma^2 B^+ (B^+)^T \quad (11)$$

$$C_u = \sigma^2 (OA)^+ O ((OA)^+ O)^T \quad (12)$$

where σ is the standard deviation of the observed data. The covariance matrices describe the uncertainties in the model parameters and its standard errors are given by the diagonal elements of the covariance matrix.

3. Application to the Kalabagh area

3.1. Regional physiography and seismicity

The study area in the geological context comprises the potwar/Hazara fold belt, the Salt Range, the Surghar Range, the Mianwali depression and the northern terminus of Khisor-Marwat Ranges (Fig. 1). Sedimentary rocks of Pliocene and Miocene are distributed throughout the area comprising mostly of sandstone, clay stone, silt stone and gravel beds. As the area is monocline so the rock strata have very low dips, generally of the order of 3 to 5 degree towards north, while the strike ranges from N75°W at the left bank to N55°E at the right bank of the Indus river in the north east of Kalabagh town. This gradual change in the strike direction is due to regional and tectonic features of the Kalabagh

region. The area is underlain by the upper part of the Middle Siwalik formation along with river channel, terrace and nala deposits (Kazmi and Jan, 1997).

In the Potwar basin deformation of considerable magnitude affected the entire area at the end of the Tertiary era resulting in development of folds and numerous faults in the region. The formation pattern has been complicated by the plasticity of the Middle Eocene formation and the Cambrian saline series.

The deformation features include gentle folds, thrust and wrench faults resulting from the late Paleocene/Pleistocene orogeny. The most recent uplift folded the Siwaliks to present position and resulted in their high dip, some degree of indurations and displaced them along a series of thrust faults (McDougal and Khan, 1990). A very low seismicity level was observed in this area during the period of study. This seismicity does not seem generally related to a particular tectonic structure but rather to a condition of general compressional stress in the area.

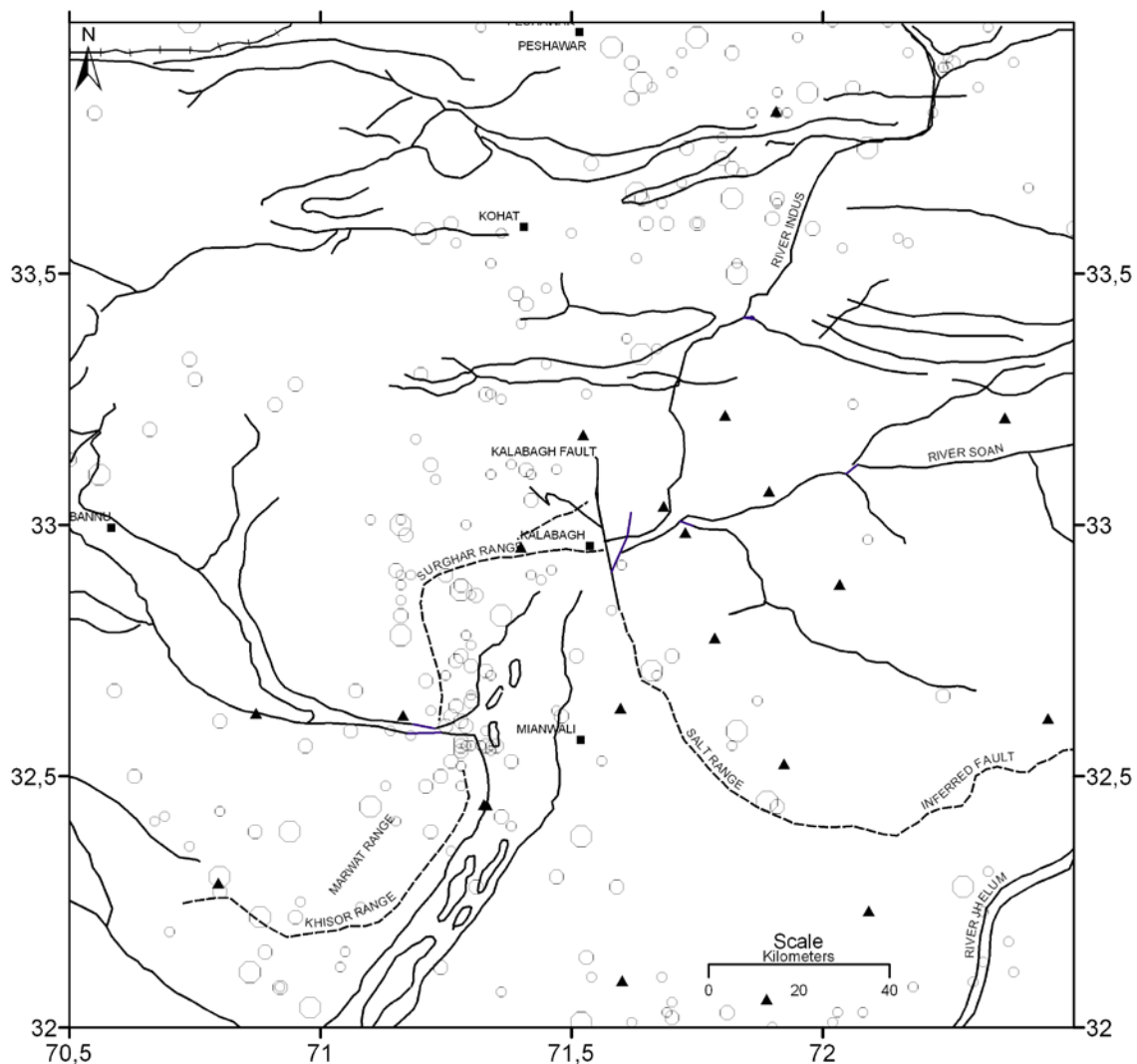


Fig. 1. Distribution of micro seismic network stations (triangles) and seismicity with magnitude ≥ 2.5 around the Kalabagh area with respect to main cities (circles).

The Salt Range is generally oriented east-west but in the western terminus it changes trend from north-northwest to south-southeast. It is essentially a faulted and folded monocline rising to the south with a marked scarp and dipping gently into the Potwar Tertiary basin to the north. The frontal portion of the range is generally thought to be formed by a thrust fault and the faults found within the Salt Range are predominantly of reverse type with some low angle thrust faults and small number of normal faults. The microseismic activity may be perhaps related to superficial deformation (depth generally less than 20 km) due to thrust mechanism. The Surghar Range, which is an extension of Salt Range, has complex structure and this complexity is probably related to a deeper contact between the Precambrian basement and the thrust units (Gee, 1980; McDougal and Khan, 1990). The eastern part appears to be composed of several enechelon strike-slip faults. One of these, the Kalabagh fault, is evident on satellite imagery, as well as being marked in the field by a prominent valley (Kazmi, 1979; McDougal and Khan, 1990). A concentration of low magnitude events has been observed in the southern part of Kalabagh fault perhaps that coalesces with a small near by strike slip fault in the vicinity of Pai Khel town and also the southwestern part of the Surghar Range.

3.2. Input data

The data used here were recorded at the central recording Lab. of Micro Seismic Studies Programme (MSSP), Islamabad. A network of about twenty telemetered seismic stations was initially installed over an area of about 100 km by 100 km to monitor the seismicity around the Kalabagh town (Fig. 1). The hypocentral parameters were determined by using earthquake location program Hypo71 (Lee and Lahr, 1975) with the assumed crustal velocity model shown in Table 1 and considering V_p/V_s ratio as 1.75. There were about 102 events with magnitude ≥ 2.5 , selected among the many events routinely located in this region, satisfying the criteria: i) the events were recorded at four or more stations, ii) they were located inside the network, iii) the travel times having residuals greater than 0.7s were discarded. The final data set has 94 events with

a total of 1036 observations recorded in the time interval of March 1981 to September 1990. The location of the epicenters is given in Figure 1 and depth distribution is shown in Figure 2.

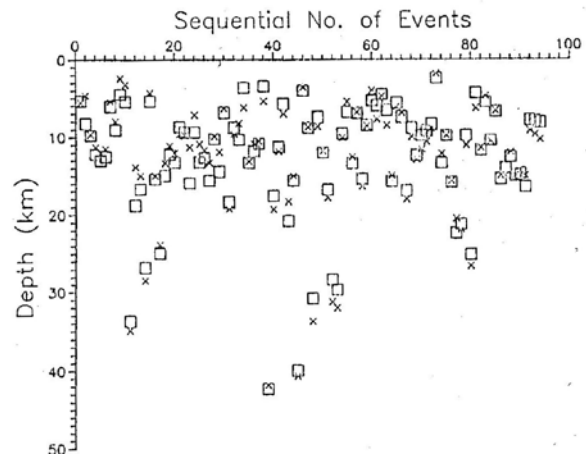


Fig. 2. Focal depth versus Sequential number of events. Crosses denote the initial depths of the events while the squares denote their relocated depth.

3.3. Velocity structure

The selection of appropriate layer thicknesses and the accuracy of observed arrival times play an important role in the inversion results and their resolution. In such inversions, the velocity structure is divided into a certain number of layers or blocks depending upon the nature of the model. The blocks sizes or the layer thicknesses are assumed on the basis of independent geophysical and geological information prior to the inversion process. When there is little information about a certain region, small blocks or layer thicknesses are assumed to obtain velocity structure as accurate as possible.

In practice, the model parameters are chosen in such a way that they can be realistically resolved by the data. The damping conditions by adjusting Θ^2 in Eq. (5), the eventual instabilities are suppressed in the inversion. In our case we have chosen the damping factor Θ^2 as 0.025 i.e. 2.5% of the maximum singular value of S_i , in order to obtain high resolution and appropriate covariance estimates in each inversion for matrices B^+ and $(OA)^+$.

The initial velocity model, as in Table 1, is used for the inversion. The residuals obtained from this model were approximately all negative and about 85% of them had residuals less than -0.725 s. This indicates that the initial model used is not suitable for this area due to low velocities of the layers or perhaps large thicknesses of the layers. To obtain a good normal distribution of the residuals we tried many models for the inversion by adjusting the structure parameters. Two of them, given in Table 2 and labeled as Model 1 and Model 2, have produced better results as compared to other models. The first layer thickness (minimum thickness) of the velocity structure was taken as 4.5 km with an overall uncertainty of 0.1s in arrival times. The Moho discontinuity was assigned at 35.5 km depth. After some adjustment in the layer thicknesses, Model 2 seems to be better if compared to the inversion results of the Model 1. The estimated velocities, obtained from the inversion of direct and head waves, their relative errors and the resolution matrices are given in Table 3. The maximum standard error in the P-wave velocity is 0.092 km/s while the resolution matrices are quasi identity matrices for these models. It may be seen from Figure 3 that the P-wave residuals (solid lines), obtained from the inversion of Model 2 (Table 2), are normally distributed and that the residuals from the initial Model 2 (dashed lines) have a positive skewness that produces a velocity increase in each fixed layer of the initial model in the inversion process. The inverted velocity structures are shown in Figure 4. The results in Figure 4a and Figure 4b are obtained by using ray tracing for direct as well as head waves since about one third of the arrival times are recorded at a distance of more than 100km. Figure 4c shows the result of the inversion obtained by assuming only direct waves, The initial model being the same as the one used in Figure 4b. The difference between the inversion models shown in Figure 4b and the Figure 4c are due to the head waves being used in the ray tracing.

Table 1. Crustal velocity model used in the hypocentral location.

Layer Thickness (km)	P-waves velocity (km/s)
3.000	4.100
3.000	4.500
3.500	5.100
4.000	5.400
13.500	6.400
12.500	7.200
∞	8.200

Table 2. Initial velocity models for inversion

Layer Thickness (km)	P-wave velocity (km/s)	
	Model 1	Model 2
4.50	4.900	5.100
6.00	5.300	5.300
8.00	5.900	6.100
7.00	6.400	6.400
10.00	6.900	6.900
11.00	7.300	7.200

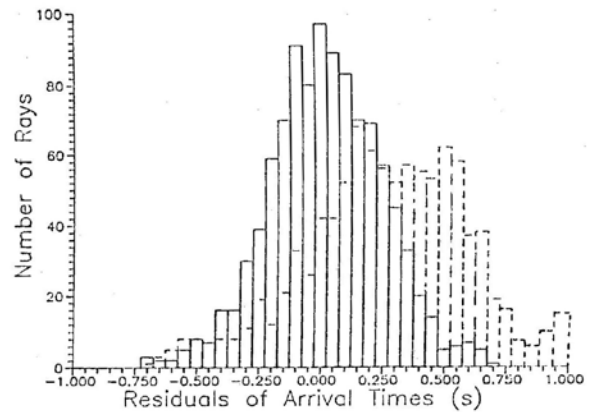


Fig. 3. Histograms of the number of earthquakes versus arrival time residuals. The dashed lines denote the results of the initial Model 2 and the solid lines the result of the relative inversion.

Table 3. Inverted velocity models

a) Direct and head waves (Model 1).

Layer Thickness Km	P-wave		Resolution matrix					
	Velocity km/s	errors km/s						
4.50	5.287	.056	.982	-.012	.001	.005	.004	.001
6.00	5.407	.056	-.012	.963	.002	.007	.006	.000
8.00	6.262	.001	.001	.002	1.000	.000	.000	.000
7.00	6.555	.085	.005	.007	.000	.901	.026	.003
10.00	6.940	.094	.004	.006	.000	.026	.816	.017
11.00	8.018	.088	.001	.000	.000	.003	.017	.927

b) Direct and head waves (Model 2).

4.50	5.334	.039	.998	-.001	.000	.001	.000	.000
6.00	5.565	.053	-.001	.993	.001	.002	.001	.000
8.00	6.268	.031	.000	.001	.999	.001	.000	.000
7.00	6.573	.083	.001	.002	.001	.967	.010	.002
10.00	6.940	.091	.000	.001	.000	.010	.950	.000
11.00	8.003	.092	.000	.000	.000	.002	.006	.961

c) Direct waves only

4.50	6.010	.029	.999	.000	.000	.000	.000	.000
6.00	6.265	.015	.000	1.000	.000	.000	.000	.000
8.00	6.414	.019	.000	.000	1.000	.000	.000	.000
7.00	6.785	.067	.000	.000	.000	.961	.009	.005
10.00	7.175	.066	.000	.000	.000	.009	.964	.012
11.00	7.906	.090	.000	.000	.000	.005	.012	.738

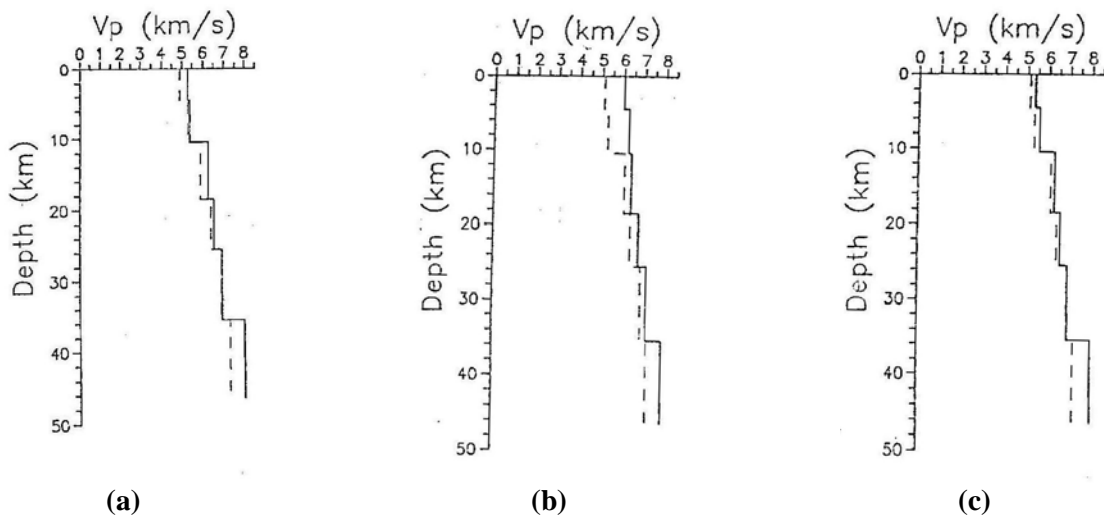


Fig. 4. The inverted velocity structure using the arrival time data of the events. The dashed lines are the initial velocity and the solid lines are the inverted velocity. (a) and (b) are the results of different initial velocity models using ray tracing for both direct and head waves; (c) is the result for direct waves only, the initial velocity model being the same as in (b).

The spatial distribution of the hypocenters is too dense to distinguish the variations between the final hypocentral parameters and the initial ones. In order to have a general idea about the variation of hypocentral location, histograms of the number of earthquakes versus hypocentral parameter (origin time, epicenter, focal depth) variation are given in Figure 5. For about 90% of the events, the variations in origin times, epicenters and focal depths are less than 1.0s, 2.0 km and 2.4 km, respectively. It is found that the variations in the hypocentral locations are not very big. Most of the events (80%) in the studied area tend to lie in the depth range 5-20 km.

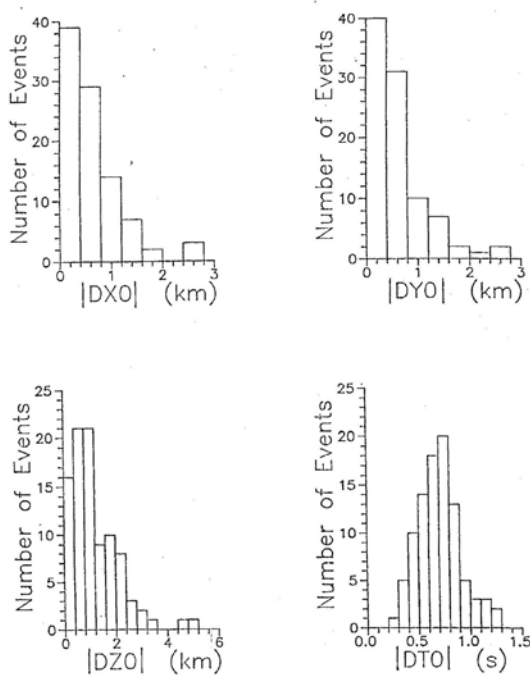


Fig. 5. Histograms of the number of earthquakes versus variations between hypocentral parameters obtained by MSSP and by present work. DT_0 is change in the origin time, DX_0 , DY_0 , DZ_0 are changes in the EW, NS and depth-components of the hypocentral location, respectively.

4. Conclusions

The simultaneous inversion of velocity structure and hypocentral location with a damped least square method is a very useful approach in studying the details of the crustal velocity structure using P-wave arrival-time data from local earthquakes recorded within the seismic network. The model parameters along with their

resolution and covariance are calculated as accurately as possible from the real observed data. The estimated velocities are 5.33 ± 0.04 and 5.56 ± 0.05 km/s in the upper crust (above a depth of 11km), 6.27 ± 0.03 and 6.57 ± 0.08 km/s in the intermediate crust and 6.94 ± 0.09 km/s in the lower part of the crust up to 35.5 km that is Moho discontinuity beneath the Kalabagh area. The simultaneous inversion of velocity structure and hypocentral location reveals that there are five layers up to Moho discontinuity under this area. Since ratio of P-wave to S-wave was taken as 1.75 in the inversion process, the corresponding shear wave velocities are 3.05 and 3.18 km/s in the upper crust, 3.58 and 3.75 km/s in the intermediate crust and 3.96 km/s in the lower part of the crust. The P-velocity just below the Moho is found to be 8.00 ± 0.09 km/s. The results also show that the velocity is constant in all layers that are used for this study. The difference in hypocentral locations is less than 2 km except for few events in which the difference is about 2-5 km. Most of the relocated events occurred between 5 and 20 km depth indicating that the active zone lies in this depth range. The application of estimated velocity structure shows improvement in hypocentral location with minimum errors.

References

- Aki, K., Lee, W.H.K., 1976. Determination of three dimensional velocity anomalies under a seismic array using first P arrival times from local earthquakes, Part I, A homogeneous initial model. *Journal of Geophysical Research*, 81, 4381-4399.
- Aki, K., Richards, P., 1980. *Methods of quantitative seismology*. Freeman, San Francisco, California.
- Crosson, R.S., 1976a. Crustal structure modeling of earthquake data, Part 1. Simultaneous least squares estimation of hypocenter and velocity parameters. *Journal of Geophysical Research*, 81, 3036-3046.
- Crosson, R.S., 1976b. Crustal structure modeling of earthquake data, Part 2. Velocity structure of the Puget Sound region, Washington. *Journal of Geophysical Research*, 81, 3047-3053.
- Gee, E.R., 1980. Salt Range series, Pakistan geological map at 1:50000, six-sheet directorate of overseas survey, UK.

- Kazmi, A.H., 1979. Active fault system in Pakistan. *Geodynamics of Pakistan*. In: Farah, A., Dejong, K. (Eds.), Geological Survey of Pakistan, Quetta, Pakistan, 285-294.
- Kazmi, A.H., Jan M.Q., 1997. *Geology and tectonics of Pakistan*. Graphic Publishers, Karachi, Pakistan.
- Lee, W.H.K., Lahr, J.C., 1975. HYPO71 (revised): A computer program for determining hypocenter, magnitude, and first motion pattern of local earthquakes. U.S. Geological Survey. Open-File Report, 75-311.
- Lee, W.H.K., Stewart, S.W., 1981. *Principles and applications of micro earthquake*. Network academic press, USA.
- Levenberg, K., 1944. A method for the solution of certain non-linear problems in least squares. *Quarterly Journal of Applied Mathematics and computation*, 2, 164-168.
- Mao, W.J., 1989. *Deformazione crostale ed inversione dei dati sismici nello studio dell'area sismica del Friuli*. Unpublished Ph.D. thesis, University of Trieste, Italy.
- Marquardt, D.W., 1963. An algorithm for least-square estimation of nonlinear parameters, *Indian Journal of Applied Mathematics and Computation*, 11, 431-441.
- McDougal, J.W., Khan, S.H., 1990. Strike slip faulting in a foreland fold- thrust belt: the Kalabagh Fault and western Salt Range, Pakistan. *Tectonics*, 9, 1061-1075.
- Menke, W., 1984. *Geophysical data analysis: Discrete inverse theory*. Academic Press, San Diego, California, USA.
- Pavlis, G.L., Booker, J.R., 1980. The mixed discrete continuous inverse problem: Application to the simultaneous determination of earthquake hypocenters and velocity structure. *Journal of Geophysical Research*, 85, 4801-4810.
- Spencer, C., Gubbins, D., 1980. Travel-time inversion for simultaneous earthquake location and velocity structure determination in laterally varying media. *Geophysical Journal of the Royal Astronomical Society*, 63, 95-116.
- Thurber, C.H., Aki, K., 1987. Three dimensional seismic imaging. *Annual Review Journal of Earth and Planetary Science letter*, 15, 115-139.
- Wadia, D.N., 1976. *Geology of India*. McGraw Hill, New Delhi, India.
- Wiggins, R.A., 1972. The general linear inverse problem: Implication of surface waves and free oscillations for earth structure. *Journal of Geophysical Research, Space Physics*, 10, 251-285.